A Nonconventional Archaeal Fluorinase Identified by in Silico Mining for Enhanced Fluorine Biocatalysis

Pardo, Isabel; Bednar, David; Calero, Patricia; Volke, Daniel C.; Damborský, Jiří; Nikel, Pablo I.

Published in:
ACS Catalysis

Link to article, DOI:
10.1021/acscatal.2c01184

Publication date:
2022

Document Version
Publisher's PDF, also known as Version of record

ACS Catalysis

pubs.acs.org/acscatalysis Letter

A Nonconventional Archaeal Fluorinase Identified by In Silico Mining for Enhanced Fluorine Biocatalysis

Isabel Pardo, David Bednar, Patricia Calero, Daniel C. Volke, Jiří Damborský, and Pablo I. Nikel*

Cite This: *ACS Catal.* 2022, 12, 6570−6577 Read Online

ACCESS | Metrics & More | Article Recommendations | Supporting Information

ABSTRACT: Fluorinases, the only enzymes known to catalyze the transfer of fluorine to an organic molecule, are essential catalysts for the biological synthesis of valuable organofluorines. However, the few fluorinases identified so far have low turnover rates that hamper biotechnological applications. Here, we isolated and characterized putative fluorinases retrieved from systematic in silico mining and identified a nonconventional archaeal enzyme from *Methanosaeta* sp. that mediates the fastest S_N2 fluorination rate reported to date. Furthermore, we demonstrate enhanced production of fluoronucleotides in vivo in a bacterial host engineered with this archaeal fluorinase, paving the way toward synthetic metabolism for efficient biohalogenation.

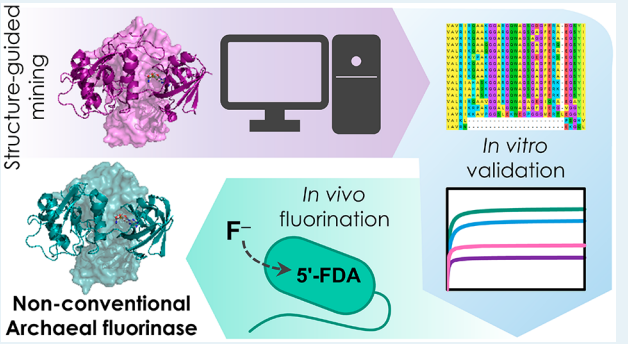

KEYWORDS: *fluorinase, fluorine, organofluorine, synthetic biology, biocatalysis, metabolic engineering, synthetic metabolism*

Fluorinated organic compounds (organofluorines), containing at least one fluorine (F) atom, are chemicals of enormous industrial interest[1,2]—as evidenced by their increasing prevalence in pharmaceuticals (almost one-third of the pharma molecules in the market contain F) and agrochemicals.[3−5] The unique physicochemical properties of F endow organofluorines with advantageous properties with respect to their nonfluorinated counterparts, e.g. increased chemical stability or improved bioavailability.[6] However, the abundance of human-made organofluorines contrasts with their relative scarcity in Nature.[7,8] 5′-Fluoro-5′-deoxyadenosine (5′-FDA) synthase, or fluorinase (FlA), is the only one enzyme known to naturally catalyze the formation of the C−F bond, which requires a high activation energy for desolvation of the fluoride ion (F^-). This enzyme, originally identified in *Streptomyces cattleya*,[9,10] catalyzes the S_N2 transfer of F^- to the C5′ of the essential methyl donor *S*-adenosyl-L-methionine (SAM), thereby generating 5′-FDA and L-methionine (L-Met) as products[11] (step I in Scheme 1). Since the discovery of FlA in 2003, only six other fluorinases have been reported in the literature, all of them sourced from actinomycetes.[12−14] A chlorinase, catalyzing 5′-chloro-5′-deoxyadenosine (5′-ClDA) synthesis and closely related to FlAs, has also been identified in the marine actinomycete *Salinispora tropica*[15] (step II in Scheme 1). FlA from *S. cattleya* is capable of catalyzing the chlorination reaction as well, albeit much less efficiently than fluorination.[16] Conversely, SalL, the chlorinase of *S. tropica*, cannot catalyze the formation of C−F bonds. This activity difference has been attributed to the presence of a 23-residue loop, present in all known FlAs but absent in SalL.[17] It was hypothesized that this loop, located near the catalytic site, could influence halide specificity by modifying the architecture of the binding pocket.[18]

Considering the environmentally harsh conditions currently required for the chemical synthesis of organofluorines, FlAs are promising biocatalysts for "green" production[19] of new-to-Nature, bioderived organofluorines and for the implementation of synthetic metabolism with fluorinated intermediates in living cells.[20−22] However, all known FlAs are poor biocatalysts,[23] with turnover rates <1 min^{-1}. So far, the handful of protein engineering efforts aimed at the improvement of FlA activity have had limited success.[24−26] Furthermore, these studies mostly relied on employing surrogate substrates, for example, 5′-ClDA, to select for enzyme variants with improved transhalogenation activity[25] (see steps III and I in Scheme 1). This strategy hampers the applicability of FlAs in a consolidated, whole-cell bioprocess where only F^- and an appropriate carbon substrate would be supplied as feedstock to support de novo biofluorination.[27]

Genome-wide databases are a rich source of potentially valuable enzymes,[28] yet their continuous, exponential expansion makes the selection of catalytically attractive candidates challenging. The *EnzymeMiner* platform[29] has been recently developed to address this issue as an interactive

Received: March 8, 2022
Revised: May 15, 2022
Published: May 19, 2022

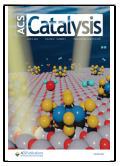

Scheme 1. Fluorometabolite Biosynthesis Pathways and Reactions Catalyzed by Fluorinase/Chlorinase[a]

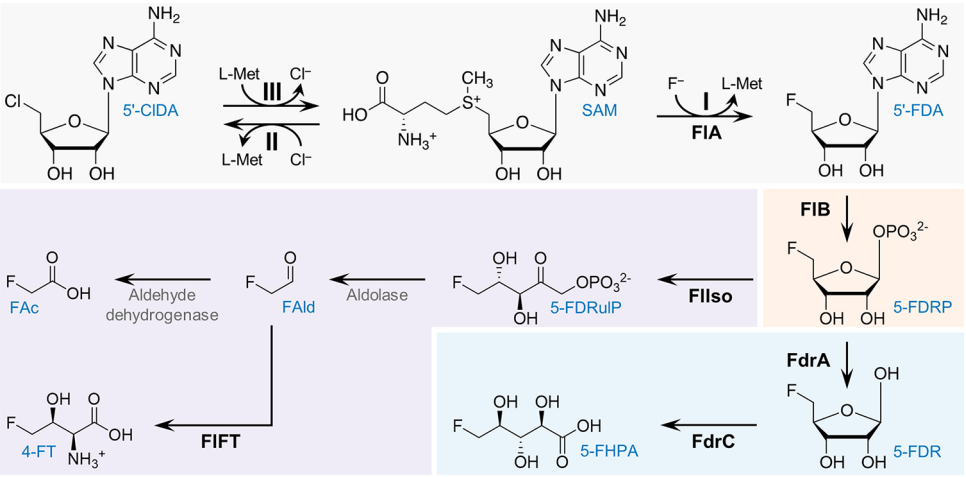

[a]Reactions catalyzed by fluorinase/chlorinase are indicated in gray: (I) forward fluorination reaction, (II) forward chlorination reaction, and (III) reverse chlorination reaction. The common step in fluorometabolite biosynthetic pathways is shaded in orange. The canonical fluoroacetate and 4-fluoro-L-threonine biosynthetic pathway are show in purple. The 5′-fluoro-5′-deoxy-D-ribose biosynthetic route is indicated in light blue. Compound abbreviations (blue): 5′-ClDA, 5′-chloro-5′-deoxyadenosine; SAM, *S*-adenosyl-L-methionine; 5′-FDA, 5′-fluoro-5′-deoxyadenosine; 5-FDRP, 5′-fluoro-5′-deoxy-D-ribose 1-phosphate; 5-FDRulP, 5-fluoro-5-deoxy-D-ribulose 1-phosphate; FAld, fluoroacetaldehyde; FAc, fluoroacetate; 4-FT, 4-fluoro-L-threonine; 5-FDR, 5′-fluoro-5′-deoxy-D-ribose; 5-FHPA, 5-fluoro-2,3,4-trihydroxypentanoic acid. Enzyme abbreviations (black bold): FlA, fluorinase; FlB, 5′-fluoro-5′-deoxyadenosine phosphorylase; FlIso, 5-fluoro-5-deoxy-D-ribose 1-phosphate isomerase; FlFT, 4-fluoro-L-threonine transaldolase; FdrA, 5-fluoro-5-deoxy-D-ribose 1-phosphate phosphoesterase; and FdrC, 5-fluoro-5-deoxy-D-ribose dehydrogenase.

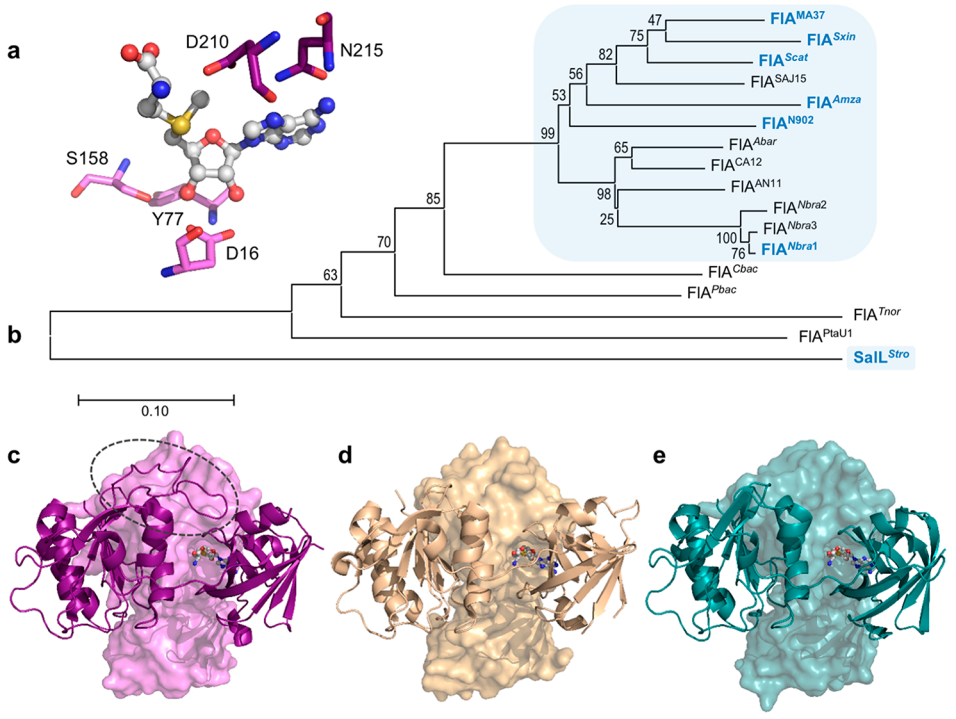

Figure 1. Putative fluorinases identified by genome mining. (a) Residues specified as essential for the *EnzymeMiner* search, based on the crystal structure of FlA^{MA37} (PDB ID 5B6I). The SAM substrate is shown as a ball-and-stick representation. (b) Phylogenetic tree of retrieved fluorinase sequences obtained using the MEGAX software,[31] inferred using the Neighbor-Joining method with a bootstrap of 10 000 iterations. The percentage of replicate trees in which the associated taxa clustered together in the bootstrap test are shown next to the branches. The tree is drawn to scale, with branch lengths in the same units as those of the evolutionary distances used to infer the phylogenetic tree. Sequences sourced from Actinomycetes are highlighted as blue squares. Enzymes previously characterized in the literature are indicated in blue bold font. (c-e) 3D structures for FlA^{MA37} (c), wild-type $SalL^{Stro}$ (d, PDB ID 6RYZ) and FlA^{PtaU1} (e, modeled with the SWISS-MODEL Alignment Mode tool using the FlA^{Scat} crystal structure PDB ID 2 V7 V as template). The loop hypothesized to differentiate fluorinases from chlorinases is circled in a dashed gray line. Two chains from the homotrimer for each structure are shown as cartoon and surface representations, respectively.

Web site (https://loschmidt.chemi.muni.cz/enzymeminer). This user-friendly bioinformatic tool searches through databases upon submitting a sequence of at least one representative member of the target enzyme family, together with the

https://doi.org/10.1021/acscatal.2c01184
ACS Catal. 2022, 12, 6570−6577

identification of essential (i.e., catalytic) residues. *EnzymeMiner* conducts multiple database searches and accompanying calculations, which provide a set of hits and their systematic annotation based on protein solubility, possible extremophilicity, domain structures, and other structural information. These collected and calculated annotations provide users with key information needed for the selection of the most promising sequences for gene synthesis, small-scale protein expression, purification, and functional characterization.[30]

With the goal of expanding the FlA toolset for the biological production of organofluorines in engineered bacterial cell factories, here we describe the systematic screening, in vitro characterization, and in vivo implementation of hitherto unknown FlAs retrieved from genome databases. First, in an effort to identify "Nature's best" biocatalyst, the fluorinase from *Streptomyces* sp. MA37 (FlA^{MA37}) was used as the query sequence (UniProt W0W999), and the amino acid residues D16, Y77, S158, D210 and N215 were specified as essential based on their implication in catalysis and substrate binding in *EnzymeMiner* (Figure 1a). We selected this enzyme since it is one of the most efficient fluorinases reported in the literature thus far, and it has been used as template for directed evolution experiments.[12,24]

After curing out redundant sequences, 16 unique candidates were obtained (Table 1 and Figure 1b). Some of the retrieved amino acid sequences were found to be missing several *N*-terminal residues, which were added after manually curating the deposited genome sequences where the fluorinase genes had been predicted (Table S1). Out of the 16 sequences retrieved, five corresponded to fluorinases reported in the literature (thus serving as an internal quality control of the prediction routine), while nine corresponded to new putative fluorinases. Another two sequences corresponded to a site-directed mutagenesis variant of the chlorinase from *Salinispora tropica* CNB-440 (SalL; carrying point substitutions Y70T and G131S)[15] and a putative chlorinase from the archaea *Methanosaeta* sp. PtaU1.Bin055 (FlA^{PtaU1}). Both of these sequences lack the 23-residue loop previously hypothesized to differentiate fluorinases from chlorinases (Figure 1c–e).

Table 1. Putative Fluorinases Retrieved from *EnzymeMiner* Analysis Using FlA^{MA37} as the Query

name	organism and reference	ID (%)[a]
FlA^{MA37}	*Streptomyces* sp. MA37[12]	query
FlA^{Scat}	*Streptomyces cattleya*[10]	87.6%
FlA^{Sxin}	*Streptomyces xinghaiensis*[13]	86.0%
FlA^{SAJ15}	*Streptomyces* sp. SAJ15	85.0%
FlA^{N902}	*Actinoplanes* sp. N902−109[12]	80.7%
FlA^{Amza}	*Actinopolyspora mzabensis*[14]	78.9%
FlA^{Abar}	*Amycolatopsis bartoniae*	79.1%
FlA^{CA12}	*Amycolatopsis* sp. CA-128772	78.6%
FlA^{AN11}	*Goodfellowiella* sp. AN110305	77.7%
FlA^{Nbra2}	*Nocardia brasiliensis* IFM 10847	75.7%
FlA^{Nbra3}	*Nocardia brasiliensis* NCTC 11294	75.3%
FlA^{Nbra1}	*Nocardia brasiliensis* ATCC 700358[12]	75.3%
FlA^{Cbac}	*Chloroflexi* bacterium	69.3%
FlA^{Pbac}	*Peptococcaceae* bacterium CEB3	64.8%
FlA^{Tnor}	*Thermodesulforhabdus norvegica*	54.5%
FlA^{PtaU1}	*Methanosaeta* sp. PtaU1.Bin055	49.5%
$SalL^{Stro}$	*Salinispora tropica* CNB-440[15]	35.6%

[a]Sequence identity. References to known FlAs are indicated.

Notably, only four of all the retrieved sequences were not sourced from Actinobacteria. These include the putative enzymes from a *Chloroflexi* bacterium (Chloroflexi), *Peptococcaceae bacterium* CEB3 (Clostridia), *Thermosulforhabdus norvegica* (Deltaproteobacteria), and *Methanosaeta* sp. PtaU1.Bin055 (Methanomicrobia). Phylogenetic analysis of the 16S rRNA sequences of the fluorinase-encoding organisms gave a similar result to that obtained when using the fluorinase amino acid sequences, except that, expectedly, *S. tropica* groups together with the other Actinomycetes, in a clade separate from the one formed by *Streptomyces* sp. (Figure S1 and Table S2).

The genomic context of the different *flA* genes was likewise examined (Table S3). As reported for the fluorination gene clusters of *Streptomyces* sp. MA37, *N. brasiliensis*, *Actinoplanes* sp. N902−109, and *S. xinghaiensis*, all Actinomycetes harbor gene clusters resembling that of *S. cattleya*, the most studied source of *fl* genes described to date[23,32] (Figure 2). The genes *flB* (encoding a 5′-FDA phosphorylase), *flG* (encoding a response regulator), *flH* (encoding a putative cation:H^+ antiporter), and *flI* (encoding a *S*-adenosyl-L-homocysteinase) were highly conserved in all actinomycetes. Most of them also presented the genes *flIso* (5-fluoro-5-deoxy-D-ribose 1-phosphate isomerase) and *flFT* (4-fluoro-L-threonine transaldolase), involved in the synthesis of fluoroacetate and 4-fluoro-L-threonine. These are the two canonical end fluorometabolites described thus far.[1] Also, genes encoding a prolyl-tRNA synthetase-associated protein and an EamA family transporter were usually found in proximity to *flFT*. In *S. cattleya*, the products of these genes (termed *fthB* and *fthC*, respectively) play a role in detoxification by deacylation of 4-fluoro-L-threoninyl-tRNA and export of 4-fluoro-L-threonine.[33] Interestingly, *Amycolatopsis bartoniae* and *Goodfellowiella* sp. AN110305 lacked either *flIso* and *flFT* orthologues within the *fl* cluster, presenting, instead, orthologues to the *fdr* genes from *Streptomyces* sp. MA37. The genes are probably involved in the biosynthesis of 5-fluoro-2,3,4-trihydroxypentanoic acid via the fluorosugar intermediate 5-fluoro-5-deoxy-D-ribose.[34] Further biochemical activities encoded in these gene clusters include phosphoesterases, short chain dehydrogenases, dihydroxyacid dehydratases and cyclases, suggesting that the main fluorinated compounds produced by these microorganisms could be different from the canonical fluorometabolites fluoroacetate and 4-fluoro-L-threonine. Similar activities seem to be also encoded by genes in the vicinity of *flA* in *Chloroflexi* bacterium and *salL* in *S. tropica*.[35] Other genes widely distributed among the different actinomycotal clusters encoded activities related to SAM synthesis (i.e., SAM synthetase) and *S*-adenosyl-L-homocysteine degradation (i.e., *S*-adenosyl-L-homocysteinase), a competitive inhibitor of fluorinase activity.[10] As indicated above, the latter gene (*flI*) was present in all actinomycotal clusters. Since SAM and *S*-adenosyl-L-homocysteine are involved in essential cellular reactions, it is likely that these enzymes modulate the levels of these compounds during secondary metabolism, when organofluorines are actively produced.[36] Further analysis of the genes found in these *fl* clusters will provide clues as to what activities are needed to establish robust and efficient biofluorination pathways in heterologous hosts. This prospect is particularly exciting at the light of the need of novel organofluorine biosynthesis enzymes that could be sourced from environmental microbes.[1]

https://doi.org/10.1021/acscatal.2c01184
ACS Catal. 2022, 12, 6570−6577

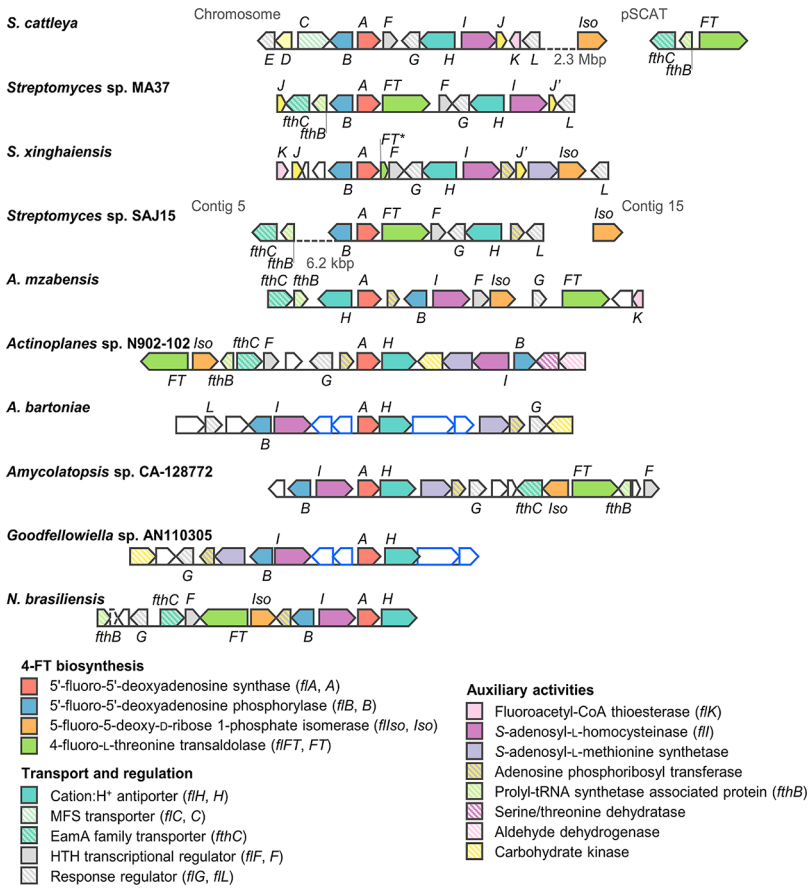

Figure 2. Fluorination gene clusters in actinomycetes. For clarity, the clusters are drawn centered on *flA* (identified as *A*) in the sense orientation. Numbers under dashed lines indicate the distance between open reading frames (ORFs) found in the same sequence entry; ORFs in separate entries are not connected by a line. Italicized letters indicate orthologues to the corresponding *fl* genes from *S. cattleya*. *J′* indicates duplicate *flJ* copies (encoding DUF190 domain-containing protein). *FT** is a truncated pseudogene homologous to *flFT*. Orthologues to *fdr* genes from *Streptomyces* sp. MA37 are indicated as white blocks with blue outlines. ORFs outlined in black represent genes with other/unknown functions. MFS, major facilitator superfamily; HTH, helix-turn-helix.

Next, the coding sequences of all FlA candidates were codon-optimized for production in *Escherichia coli* as *N*-terminal His-tag fusions (flA^{MA37}, flA^{Scat} and flA^{Sxin} had been previously codon-optimized for expression in Gram-negative hosts;[27] see also Tables S4 and S5). $SalL^{Stro}$ was not included in this experimental set since it is reportedly inactive on F^-.[15] The expression of the 16 candidate genes was initially evaluated in 96-well microtiter plate cultures. FlA^{Tnor}, FlA^{Amza}, and FlA^{Pbac} could not be obtained as soluble enzymes and were not included in further analyses. Moreover, very faint bands of the expected size were observed in SDS-PAGE of *E. coli* extracts producing either FlA^{Tnor} or FlA^{Amza}, suggesting limited expression levels or poor translation (Figure S2). Therefore, we proceeded to obtain the remaining 13 candidates in medium-scale shaken-flask cultures for His-tag purification and activity assays. The purified enzymes were incubated in the presence of increasing SAM concentrations for 1 h, after which 5′-FDA was measured by HPLC. 5′-FDA synthase activity could be detected for 12 out of the 13 candidates (Figure S3). The protein concentration was normalized for these assays, although the enzymes were recovered with varying degrees of purity due to differences in solubility—typical of proteins from high-G+C-content species when produced in a Gram-negative host.[37] Notably, the enzyme from *Methanosaeta* sp. (FlA^{PtaU1}, predicted to be a chlorinase), was one of the top performers. FlA^{SAJ15} also had high 5′-FDA synthase activity in vitro. These two enzymes had specific activities comparable to those of FlA^{MA37} and FlA^{Sxin}, with the highest catalytic efficiencies on SAM-dependent S_N2 fluorination reported to date.

FlA^{PtaU1} and FlA^{SAJ15} were selected for large-scale shaken-flask production and a more detailed biochemical characterization. Steady-state kinetics assays with 1 μM of the purified protein, varying concentrations of SAM (1.5−800 μM) and 75 mM KF revealed that both of these enzymes presented higher turnover rates (k_{cat}) than FlA^{MA37} and FlA^{Sxin} (Figure 3a and Table 2). In particular, the k_{cat} of FlA^{PtaU1} was 2.6-fold larger than that of FlA^{MA37}. Surprisingly, K_M^{SAM} values were consistently <10 μM, much lower than what had been previously reported in the literature for fluorinases.[12−14] Notably, previous studies used high enzyme concentrations (>10 μM), which impedes reaching a steady state of the reaction for substrate concentrations below 10 μM. We also used a KF concentration that ensures F^- saturation without causing any inhibitory effect (previous studies have used KF concentrations >200 mM).

To gain insight on the structural factors that could determine these differences in fluorination activity, we inspected the predicted crystal structures of FlA^{MA37}, FlA^{Sxin}, FlA^{SAJ15}, FlA^{PtaU1}, and $SalL^{Stro}$. Examination of the amino acid residues potentially interacting with SAM (at distances <5 Å) revealed important variations between the substrate binding pocket of FlA^{PtaU1} and that of the other fluorinases known to

https://doi.org/10.1021/acscatal.2c01184
ACS Catal. 2022, 12, 6570−6577

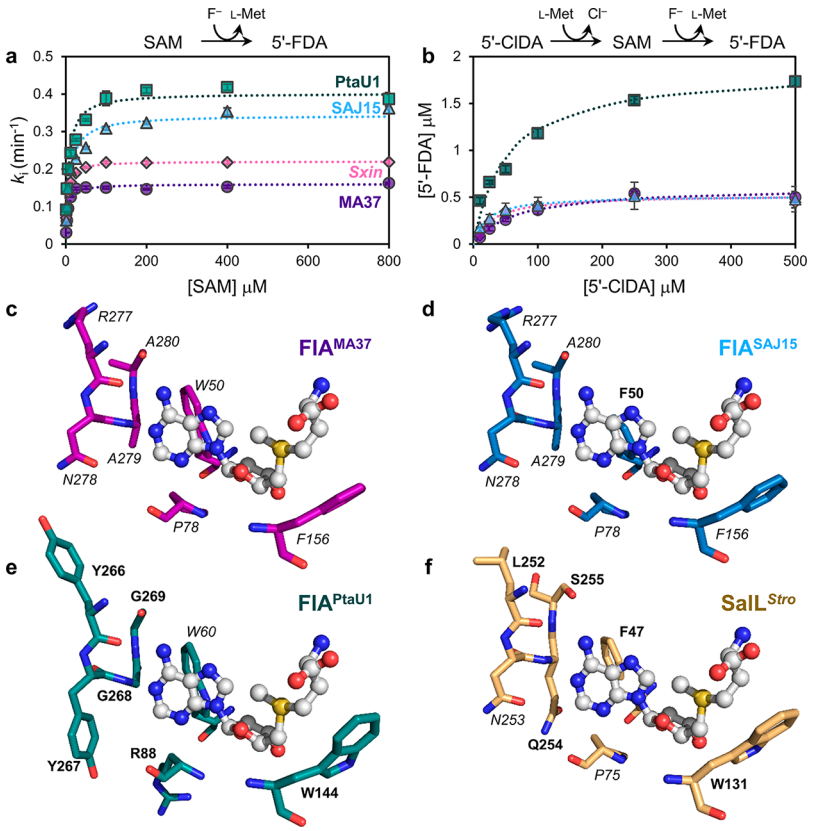

Figure 3. Biochemical characterization and residue conservation of selected fluorinases. (a) Steady-state fluorination assays using increasing SAM concentrations. Reactions were carried out at 37 °C in 50 mM HEPES buffer, pH = 7.8, with 75 mM KF. Dotted lines show fits to the Michaelis–Menten equation (R^2 > 0.95 in all cases). (b) End-point (1 h) transhalogenation assays with increasing 5′-ClDA concentrations. Reactions were carried out at 37 °C in 50 mM HEPES buffer, pH = 7.8, with 75 mM KF and 1 mM L-Met. Error bars represent standard deviations from triplicate independent assays. Symbols and color codes are kept in both panels. Simplified schematics for the corresponding reactions are shown above each panel. (c–f) Variable residues in the substrate binding pocket of FlA^{MA37} (c), FlA^{SAJ15} (d), FlA^{PtaU1} (e), and SalL^{Stro} (f). Residues that differ from those of FlA^{MA37} are labeled in bold font, whereas conserved residues are labeled in italics. FlA^{Sxin} residues are identical with those of FlA^{MA37}. The SAM substrate is shown in ball-and-stick representation.

Table 2. Michaelis–Menten Kinetic Constants of Selected Fluorinases[a]

fluorinase	K_M^{SAM} (μM)	k_{cat} (min^{-1})	k_{cat}/K_M^{SAM} (mM^{-1} min^{-1})
FlA^{MA37}	4.42 ± 0.58	0.16 ± 0.01	36.36 ± 4.82
FlA^{Sxin}	3.76 ± 0.15	0.22 ± 0.01	58.63 ± 2.63
FlA^{SAJ15}	9.62 ± 1.43	0.34 ± 0.01	35.81 ± 5.43
FlA^{PtaU1}	6.99 ± 1.06	0.41 ± 0.01	57.54 ± 8.85

[a]Assays conducted in 50 mM HEPES, pH = 7.8, with 75 mM KF and varying SAM concentrations incubated at 37 °C. Average and standard deviations are given for triplicate independent measurements.

date (Figure 3c–f). The alterations could be mapped near to the adenyl moiety of SAM, and involve the substitution of a conserved proline for an arginine residue and an RNAA motif for YYGG. This motif is found in the *C*-terminal domain of other fluorinases, which is more variable than the *N*-terminal domain and is presumably also involved in hexamer formation[38] (Figure S4). Interestingly, the catalytic features found in FlA^{PtaU1} do not resemble those of the SalL^{Stro} chlorinase, which would place FlA^{PtaU1} in a different functional group of S_N2 halogenases. Evaluating the effect of these amino acid differences in fluorinase activity will be of interest for enzyme engineering efforts.

Since FlA^{PtaU1} was predicted to be a chlorinase, we evaluated whether it was also active in S_N2-dependent addition of Cl^- to SAM. Unexpectedly, no 5′-ClDA accumulation could be detected in enzymatic reactions in which KF was replaced by KCl—in contrast to what has been reported for SalL^{Stro}.[15] Previous studies have shown that FlA^{Scat} can also catalyze the chlorination reaction.[16] However, this feature requires the simultaneous removal of L-Met or 5′-ClDA, the reaction products, since the reverse dehalogenation reaction is favored. We could observe transhalogenation on 5′-ClDA (i.e., 5′-FDA production in the presence of L-Met and F^-, steps III and I in Scheme 1; Figure 3b). Again, FlA^{PtaU1} catalytically outperformed all other fluorinases, with a 3-fold higher V_{max} value. Although we cannot rule out that FlA^{PtaU1} could also execute de novo chlorination, the 23-residue loop reportedly found in "conventional" fluorinases is not essential for the activity toward F^-.

With this background, we tested the biosynthesis of fluorometabolites *in vivo* by engineering selected fluorinases in the bacterial platform *Pseudomonas putida*, a robust chassis for engineering complex chemistries using synthetic biology tools.[39−43] We have designed a fluoride-responsive genetic circuit that enabled biofluorination in this Gram-negative host.[27] Here, this system was adapted to express either *flA*^{PtaU1} or *flA*^{SAJ15}, the best-performing fluorinases according to the kinetic parameters in Table 2. FlA^{MA37} and FlA^{Sxin} were

https://doi.org/10.1021/acscatal.2c01184
ACS Catal. 2022, 12, 6570−6577

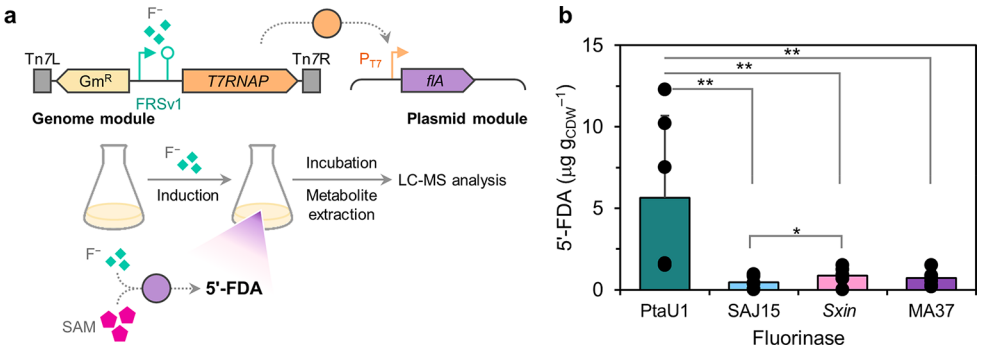

Figure 4. Engineering in vivo biofluorination in *P. putida*. (a) Schematic representation of the fluoride-responsive genetic circuit based on the T7 phage RNA polymerase (T7RNAP)[17] and workflow for the biofluorination assay. Expression of the different fluorinase genes was induced when the cultures reached an OD_{600} = 0.4−0.6 by adding NaF at 15 mM. Next, following an incubation at 30 °C for 20 h, aliquots were taken for metabolite extraction and quantification by LC-MS. Further details are provided in the Supporting Information. (b) Quantification of the intracellular 5′-FDA content in engineered *P. putida* expressing the different fluorinase genes. In this case, the intracellular 5′-FDA concentration is normalized by the cell dry weight (CDW). Black dots show individual values from six independent biological replicates, and the error bars represent standard deviations. Asterisks indicate significant differences with *p*-values <0.1 (*) or <0.05 (**) for a two-sample, one-sided Welch's *t*-test.

included in control experiments, as we have previously used them for engineering in vivo fluorination.[27] Upon inducing gene expression with NaF (which is also the substrate of the reaction of interest) and producing the fluorinases for 20 h at 30 °C, 5′-FDA biosynthesis was determined by LC-MS to evaluate de novo fluorination activity (Figure 4a). Production of 5′-FDA by engineered *P. putida* could be detected in all cases (Figure 4b). Notably, the 5′-FDA content, indicative of in vivo biofluorination, was 12-fold higher in cells expressing flA^{PtaU1} with respect to any other fluorinase gene. Fluorination activity in cell-free extracts of *P. putida* incubated for 20 h at 30 °C in the presence of exogenously added 200 μM SAM and 5 mM NaF was similar for the fluorinases tested (Figure S5), with a higher activity detected in cell-free extracts carrying FlA^{PtaU1}, the Archaeal fluorinase. In the cell-free extract assay, the final 5′-FDA concentrations detected were within the ranges previously reported.[27,38] Interestingly, no other fluorometabolites than 5′-FDA could be detected in these assays.

In conclusion, out of the 10 newly identified enzymes, the nonconventional FlA from the archaea *Methanosaeta* sp. PtaU1.Bin055 (FlA^{PtaU1}) was found to present turnover rates superior to those of all FlAs reported to date. Surprisingly, this enzyme lacks the loop that was so far hypothesized to be a differentiating feature between fluorinases and chlorinases, challenging the hypothesis that this loop is required for activity toward F^-. Engineering this nonconventional fluorinase in *P. putida* mediated the highest in vivo production of 5′-FDA described to date—and, for that matter, the highest fluorometabolite levels reported for any biological system, either natural or engineered. This work highlights the importance of systematic and efficient biocatalyst selection across the ever-expanding genomic databases, followed by careful characterization in vitro and cell factory engineering in vivo. This study also expands the known sequence diversity for fluorinase enzymes, helping in the identification of other nonintuitive sequence features. Interestingly, when the mining run was repeated with either FlA^{MA37} or FlA^{PtaU1} as query, the number of putative fluorinase sequences retrieved (24 hits) was essentially the same as obtained with the enzyme from *S. cattleya* as the template. These features will be useful for predicting protein function(s) from genomic databases annotations. Additionally, this fundamental knowledge will inform future engineering endeavors of fluorinases by rational and semirational design. Taken together, our results open avenues for the implementation of *neo*-metabolic pathways to incorporate F atoms in bacterial hosts by synthetic biology approaches.

■ ASSOCIATED CONTENT

Supporting Information

The Supporting Information is available free of charge at https://pubs.acs.org/doi/10.1021/acscatal.2c01184.

Materials and methods and supplementary figures and tables (PDF)

■ AUTHOR INFORMATION

Corresponding Author

Pablo I. Nikel − *The Novo Nordisk Foundation Center for Biosustainability, Technical University of Denmark, 2800 Kongens Lyngby, Denmark;* orcid.org/0000-0002-9313-7481; Email: pabnik@biosustain.dtu.dk

Authors

Isabel Pardo − *The Novo Nordisk Foundation Center for Biosustainability, Technical University of Denmark, 2800 Kongens Lyngby, Denmark;* Present Address: Department of Microbial and Plant Biotechnology, Centro de Investigaciones Biológicas Margarita Salas, CSIC, 28040 Madrid, Spain

David Bednar − *Loschmidt Laboratories, Department of Experimental Biology and RECETOX, Faculty of Science, Masaryk University, 601 77 Brno, Czech Republic; International Clinical Research Centre, St. Anne's University Hospital, 656 91 Brno, Czech Republic*

Patricia Calero − *The Novo Nordisk Foundation Center for Biosustainability, Technical University of Denmark, 2800 Kongens Lyngby, Denmark*

Daniel C. Volke − *The Novo Nordisk Foundation Center for Biosustainability, Technical University of Denmark, 2800 Kongens Lyngby, Denmark*

Jiří Damborský − *Loschmidt Laboratories, Department of Experimental Biology and RECETOX, Faculty of Science, Masaryk University, 601 77 Brno, Czech Republic; International Clinical Research Centre, St. Anne's University Hospital, 656 91 Brno, Czech Republic*

https://doi.org/10.1021/acscatal.2c01184
ACS Catal. 2022, 12, 6570−6577

Complete contact information is available at: https://pubs.acs.org/10.1021/acscatal.2c01184

Author Contributions

I.P. performed most of the experimental work and phylogenetic analysis, interpreted the data, and wrote the manuscript draft. P.C. and C.D.V. performed experimental work and contributed to manuscript writing. D.B. and J.D. performed in silico work and contributed to manuscript writing. P.I.N. acquired funding, conceptualized the study, supervised the work and finalized the manuscript. All authors have approved the final version of the manuscript.

Notes

The authors declare no competing financial interest.

■ ACKNOWLEDGMENTS

This work was supported by the European Union's Horizon 2020 Research and Innovation Programme under Grant Agreement No. 814418 (*SinFonia*), the Czech Ministry of Education (INBIO CZ.02.1.01/0.0/0.0/16_026/0008451), and the Czech Grant Agency (DB 20-15915Y).

■ REFERENCES

(1) Cros, A.; Alfaro-Espinoza, G.; de Maria, A.; Wirth, N. T.; Nikel, P. I. Synthetic Metabolism for Biohalogenation. *Curr. Opin. Biotechnol.* **2022**, *74*, 180−193.
(2) Walker, M. C.; Chang, M. C. Y. Natural and Engineered Biosynthesis of Fluorinated Natural Products. *Chem. Soc. Rev.* **2014**, *43* (18), 6527−6536.
(3) Harsanyi, A.; Sandford, G. Organofluorine Chemistry: Applications, Sources and Sustainability. *Green Chem.* **2015**, *17* (4), 2081−2086.
(4) Inoue, M.; Sumii, Y.; Shibata, N. Contribution of Organofluorine Compounds to Pharmaceuticals. *ACS Omega* **2020**, *5* (19), 10633−10640.
(5) Ogawa, Y.; Tokunaga, E.; Kobayashi, O.; Hirai, K.; Shibata, N. Current Contributions of Organofluorine Compounds to the Agrochemical Industry. *iScience* **2020**, *23* (9), 101467.
(6) O'Hagan, D. Understanding Organofluorine Chemistry. An Introduction to the C−F Bond. *Chem. Soc. Rev.* **2008**, *37*, 308−319.
(7) Carvalho, M. F.; Oliveira, R. S. Natural Production of Fluorinated Compounds and Biotechnological Prospects of the Fluorinase Enzyme. *Crit. Rev. Biotechnol.* **2017**, *37* (7), 880−897.
(8) Deng, H.; O'Hagan, D.; Schaffrath, C. Fluorometabolite Biosynthesis and the Fluorinase from *Streptomyces cattleya*. *Nat. Prod. Rep.* **2004**, *21* (6), 773−784.
(9) O'Hagan, D.; Schaffrath, C.; Cobb, S. L.; Hamilton, J. T.; Murphy, C. D. Biochemistry: Biosynthesis of an Organofluorine Molecule. *Nature* **2002**, *416* (6878), 279.
(10) Schaffrath, C.; Deng, H.; O'Hagan, D. Isolation and Characterisation of 5′-Fluorodeoxyadenosine Synthase, a Fluorination Enzyme from *Streptomyces cattleya*. *FEBS Lett.* **2003**, *547* (1−3), 111−114.
(11) Zhu, X.; Robinson, D. A.; McEwan, A. R.; O'Hagan, D.; Naismith, J. H. Mechanism of Enzymatic Fluorination in *Streptomyces cattleya*. *J. Am. Chem. Soc.* **2007**, *129* (47), 14597−14604.
(12) Deng, H.; Ma, L.; Bandaranayaka, N.; Qin, Z.; Mann, G.; Kyeremeh, K.; Yu, Y.; Shepherd, T.; Naismith, J. H.; O'Hagan, D. Identification of Fluorinases from *Streptomyces* sp Ma37, *Nocardia brasiliensis*, and *Actinoplanes* sp N902−109 by Genome Mining. *ChemBioChem.* **2014**, *15* (3), 364−368.
(13) Ma, L.; Li, Y.; Meng, L.; Deng, H.; Li, Y.; Zhang, Q.; Diao, A. Biological Fluorination from the Sea: Discovery of a SAM-Dependent Nucleophilic Fluorinating Enzyme from the Marine-Derived Bacterium *Streptomyces xinghaiensis* NRRL B24674. *RSC Adv.* **2016**, *6*, 27047−27051.
(14) Sooklal, S. A.; de Koning, C.; Brady, D.; Rumbold, K. Identification and Characterisation of a Fluorinase from *Actinopolyspora mzabensis*. *Protein Expr. Purif.* **2020**, *166*, 105508.
(15) Eustáquio, A. S.; Pojer, F.; Noel, J. P.; Moore, B. S. Discovery and Characterization of a Marine Bacterial SAM-Dependent Chlorinase. *Nat. Chem. Biol.* **2008**, *4* (1), 69−74.
(16) Deng, H.; Cobb, S. L.; McEwan, A. R.; McGlinchey, R. P.; Naismith, J. H.; O'Hagan, D.; Robinson, D. A.; Spencer, J. B. The Fluorinase from *Streptomyces cattleya* is Also a Chlorinase. *Angew. Chem., Int. Ed. Engl.* **2006**, *45* (5), 759−762.
(17) Deng, H.; O'Hagan, D. The Fluorinase, the Chlorinase and the Duf-62 Enzymes. *Curr. Opin. Chem. Biol.* **2008**, *12* (5), 582−592.
(18) Pereira, P. R. M.; Araújo, J. O.; Silva, J. R. A.; Alves, C. N.; Lameira, J.; Lima, A. H. Exploring Chloride Selectivity and Halogenase Regioselectivity of the Sall Enzyme through Quantum Mechanical/Molecular Mechanical Modeling. *J. Chem. Inf. Model.* **2020**, *60* (2), 738−746.
(19) Hauer, B. Embracing Nature's Catalysts: A Viewpoint on the Future of Biocatalysis. *ACS Catal.* **2020**, *10* (15), 8418−8427.
(20) Martinelli, L.; Nikel, P. I. Breaking the State-of-the-Art in the Chemical Industry with New-to-Nature Products *via* Synthetic Microbiology. *Microb. Biotechnol.* **2019**, *12* (2), 187−190.
(21) Nieto-Domínguez, M.; Nikel, P. I. Intersecting Xenobiology and *Neo*-Metabolism to Bring Novel Chemistries to Life. *ChemBioChem.* **2020**, *21* (18), 2551−2571.
(22) Walker, M. C.; Thuronyi, B. W.; Charkoudian, L. K.; Lowry, B.; Khosla, C.; Chang, M. C. Expanding the Fluorine Chemistry of Living Systems Using Engineered Polyketide Synthase Pathways. *Science* **2013**, *341* (6150), 1089−1094.
(23) O'Hagan, D.; Deng, H. Enzymatic Fluorination and Biotechnological Developments of the Fluorinase. *Chem. Rev.* **2015**, *115* (2), 634−649.
(24) Sun, H.; Yeo, W. L.; Lim, Y. H.; Chew, X.; Smith, D. J.; Xue, B.; Chan, K. P.; Robinson, R. C.; Robins, E. G.; Zhao, H.; Ang, E. L. Directed Evolution of a Fluorinase for Improved Fluorination Efficiency with a Non-Native Substrate. *Angew. Chem., Int. Ed.* **2016**, *55* (46), 14277−14280.
(25) Sun, H.; Zhao, H.; Ang, E. L. A Coupled Chlorinase−Fluorinase System with a High Efficiency of *trans*-Halogenation and a Shared Substrate Tolerance. *Chem. Commun.* **2018**, *54* (68), 9458−9461.
(26) Thomsen, M.; Vogensen, S. B.; Buchardt, J.; Burkart, M. D.; Clausen, R. P. Chemoenzymatic Synthesis and *in situ* Application of *S*-Adenosyl-L-Methionine Analogs. *Org. Biomol. Chem.* **2013**, *11* (43), 7606−7610.
(27) Calero, P.; Volke, D. C.; Lowe, P. T.; Gotfredsen, C. H.; O'Hagan, D.; Nikel, P. I. A Fluoride-Responsive Genetic Circuit Enables *in vivo* Biofluorination in Engineered *Pseudomonas putida*. *Nat. Commun.* **2020**, *11* (1), 5045.
(28) Scherlach, K.; Hertweck, C. Mining and Unearthing Hidden Biosynthetic Potential. *Nat. Commun.* **2021**, *12* (1), 3864.
(29) Hon, J.; Borko, S.; Stourac, J.; Prokop, Z.; Zendulka, J.; Bednar, D.; Martinek, T.; Damborský, J. *EnzymeMiner*: Automated Mining of Soluble Enzymes with Diverse Structures, Catalytic Properties and Stabilities. *Nucleic Acids Res.* **2020**, *48* (W1), W104−W109.
(30) Vanacek, P.; Sebestova, E.; Babkova, P.; Bidmanova, S.; Daniel, L.; Dvořák, P.; Stepankova, V.; Chaloupkova, R.; Brezovsky, J.; Prokop, Z.; Damborský, J. Exploration of Enzyme Diversity by Integrating Bioinformatics with Expression Analysis and Biochemical Characterization. *ACS Catal.* **2018**, *8* (3), 2402−2412.
(31) Kumar, S.; Stecher, G.; Li, M.; Knyaz, C.; Tamura, K. *Mega X*: Molecular Evolutionary Genetics Analysis across Computing Platforms. *Mol. Biol. Evol.* **2018**, *35* (6), 1547−1549.
(32) Huang, F.; Haydock, S. F.; Spiteller, D.; Mironenko, T.; Li, T. L.; O'Hagan, D.; Leadlay, P. F.; Spencer, J. B. The Gene Cluster for Fluorometabolite Biosynthesis in *Streptomyces cattleya*: A Thioesterase Confers Resistance to Fluoroacetyl-Coenzyme A. *Chem. Biol.* **2006**, *13* (5), 475−484.

(33) McMurry, J. L.; Chang, M. C. Y. Fluorothreonyl-tRNA Deacylase Prevents Mistranslation in the Organofluorine Producer *Streptomyces cattleya*. *Proc. Natl. Acad. Sci. U.S.A.* **2017**, *114* (45), 11920−11925.
(34) Ma, L.; Bartholomé, A.; Tong, M. H.; Qin, Z.; Yu, Y.; Shepherd, T.; Kyeremeh, K.; Deng, H.; O'Hagan, D. Identification of a Fluorometabolite from *Streptomyces* sp. MA37: (2*R*3*S*4*S*)-5-Fluoro-2,3,4-Trihydroxypentanoic Acid. *Chem. Sci.* **2015**, *6*, 1414.
(35) Eustáquio, A. S.; McGlinchey, R. P.; Liu, Y.; Hazzard, C.; Beer, L. L.; Florova, G.; Alhamadsheh, M. M.; Lechner, A.; Kale, A. J.; Kobayashi, Y.; Reynolds, K. A.; Moore, B. S. Biosynthesis of the Salinosporamide A Polyketide Synthase Substrate Chloroethylmalonyl-Coenzyme A from *S*-Adenosyl-L-Methionine. *Proc. Natl. Acad. Sci. U.S.A.* **2009**, *106* (30), 12295−12300.
(36) Zhao, C.; Li, P.; Deng, Z.; Ou, H. Y.; McGlinchey, R. P.; O'Hagan, D. Insights into Fluorometabolite Biosynthesis in *Streptomyces cattleya* DSM46488 through Genome Sequence and Knockout Mutants. *Bioorg. Chem.* **2012**, *44*, 1−7.
(37) Boël, G.; Letso, R.; Neely, H.; Price, W. N.; Wong, K. H.; Su, M.; Luff, J.; Valecha, M.; Everett, J. K.; Acton, T. B.; Xiao, R.; Montelione, G. T.; Aalberts, D. P.; Hunt, J. F. Codon Influence on Protein Expression in *E. coli* Correlates with mRNA Levels. *Nature* **2016**, *529* (7586), 358−363.
(38) Kittilä, T.; Calero, P.; Fredslund, F.; Lowe, P. T.; Tezé, D.; Nieto-Domínguez, M.; O'Hagan, D.; Nikel, P. I.; Welner, D. H. Oligomerization Engineering of the Fluorinase Enzyme Leads to an Active Trimer That Supports Synthesis of Fluorometabolites *in vitro*. *Microb. Biotechnol.* **2022**, *15* (5), 1622−1632.
(39) Wirth, N. T.; Nikel, P. I. Combinatorial Pathway Balancing Provides Biosynthetic Access to 2-Fluoro-*cis*,*cis*-Muconate in Engineered *Pseudomonas putida*. *Chem. Catal.* **2021**, *1* (6), 1234−1259.
(40) Nikel, P. I.; de Lorenzo, V. *Pseudomonas putida* as a Functional *chassis* for Industrial Biocatalysis: From Native Biochemistry to *Trans*-Metabolism. *Metab. Eng.* **2018**, *50*, 142−155.
(41) Volke, D. C.; Calero, P.; Nikel, P. I. Pseudomonas putida. *Trends Microbiol.* **2020**, *28* (6), 512−513.
(42) Sánchez-Pascuala, A.; Fernández-Cabezón, L.; de Lorenzo, V.; Nikel, P. I. Functional Implementation of a Linear Glycolysis for Sugar Catabolism in *Pseudomonas putida*. *Metab. Eng.* **2019**, *54*, 200−211.
(43) Bitzenhofer, N. L.; Kruse, L.; Thies, S.; Wynands, B.; Lechtenberg, T.; Rönitz, J.; Kozaeva, E.; Wirth, N. T.; Eberlein, C.; Jaeger, K. E.; Nikel, P. I.; Heipieper, H. J.; Wierckx, N.; Loeschcke, A. Towards Robust *Pseudomonas* Cell Factories to Harbour Novel Biosynthetic Pathways. *Essays Biochem.* **2021**, *65* (2), 319−336.

https://doi.org/10.1021/acscatal.2c01184
ACS Catal. 2022, 12, 6570−6577